EFFECTS OF WATER DEPTH ON STOPPING MANEUVER USING CFD NUMERICAL SIMULATION

CHENGUANG SUN[1], JIANHUA WANG[2], DECHENG WAN[*]

State Key Laboratory of Ocean Engineering, School of Naval Architecture, Ocean and Civil Engineering, Shanghai Jiao Tong University, Collaborative Innovation Center for Advanced Ship and Deep-Sea Exploration, Shanghai 200240
Corresponding Author: dcwan@sjtu.edu.cn

Keywords: *Stopping maneuver; Shallow water; naoe-FOAM-SJTU solver; Overset grid method*

As the increasingly-crowded ports and waterways, stopping ability is critical to the safety of ship maneuvering. When a ship travels in shallow water, maritime disasters such as collision and grounding occur more easily than in open waters. Therefore, it is necessary to study the behaviour of large marine vehicles in shallow water. In this paper, naoe-FOAM-SJTU solver with a hierarchy of bodies like hull, propeller and rudder using overset grid technology based on open source CFD platform OpenFOAM developed by Wan Decheng's research team in Shanghai Jiao Tong University is used to numerically investigate complex ship motion problem in stopping manuever. The simulation starts from the steady state of self-propulsion. Then the propeller is controlled to a reverse speed to carry on the stopping manuever, both in shallow and deep water. Detail information such as longitudinal and lateral distance, ship velocity and other relative parameters during stopping manuever are presented. Shallow water effects on stopping manuever is analysed through comparison of trajectory, forces, pressure distribution and flow field situation. In conclusion, several suggestions are provided to the choice of safe stopping methods in shallow water.

Introduction

In recent years, ships tend to become larger for reducing the cost of shipping and improving the transport efficiency. Since the large size worsens the manoeuvrability, accidents can easily occur in shallow water area such as crowded ports and channels. Therefore, it is significant to study the stopping ability of large ships in shallow water to prevent the ship from collision and grounding and to ensure the safety of the ship sailing near the port.

Generally, reversing the propeller is still the most common operation when a large ship needs to brake. In the procedure of the stopping manuever, the bow will turn left or right by the side forces at the aft caused by reversing propeller. The existence of the transversal force caused by reversing propeller is determined by SmittL[1] through a ship model test. Good stopping ability means minimum stopping distance, horizontal distance and yaw motion.

Among several approaches to predict ship maneuverability, direct numerical simulation is the most accurate way to reappear the real flow field during ship maneuvering motion. Using overset grid technique to solve the problem of large amplitude motion of the ship is currently the mainstream methods. Sakamoto[2] simulated the static and dynamic PMM test and gave the corresponding verification work by ship hydrodynamics software CFDShip-Iwoa Ver. 4. By solving the unsteady RANS equation, Carrica[3] carried out the numerical simulation of Z type control test of the DTMB5512 ship model. Professor Wan Decheng's research team in Shanghai Jiao Tong University developed naoe-FOAM-SJTU solver[4] based on open source CFD software OpenFOAM, which achieved great results in simulating the motion of ships and floating structures. By using the solver, Wang[5] realized the numerical simulation of the self-propulsion of ONRT in the wave.

In this paper, the author uses naoe-FOAM-SJTU solver based on overset grid technique to simulate the stopping maneuver both in shallow and deep water, predicting the vertical distance, the horizontal distance, and other parameters. Detailed analysis and comparison of the pressure distribution and the flow field around the ship are presented. The prediction can provide reference when designing a ship or choosing a stopping method.

Mathematical and numerical modelling

The computations are performed with CFD solver naoe-FOAM-SJTU. The fluid control equation is presented as an unsteady two phase incompressible RANS equation, which is as follows:

$$\nabla \cdot U = 0 \tag{1}$$

$$\frac{\partial \rho U}{\partial t} + \nabla \cdot [\rho(U - U_g)U] = -\nabla p_d - g \cdot x\nabla\rho + \nabla \cdot (\mu_{eff}\nabla U) + (\nabla U) \cdot \nabla\mu_{eff} + f_\sigma \tag{2}$$

where U is the fluid velocity field; U_g is the grid velocity; p_d is the dynamic pressure; ρ is the mixture density of the two-phase fluid; g is the gravitation acceleration; μ_{eff} is the effective dynamic viscosity; f_σ is the surface tension term.

In this paper, the SST K-W turbulence model is used to solve the RANS equation, in which k is the turbulent kinetic energy of the fluid particle and w is the characteristic dissipation rate. Turbulence model like this will not be affected by the free surface, but will also ensure the accuracy and reliability of the solution near the wall. A VOF approach with the bounded compression technique is used to capture free surface [6]. The transport equation is defined as:

$$\frac{\partial \alpha}{\partial t} + \nabla \cdot [\rho(U - U_g)\alpha] + \nabla \cdot [U_r(1 - \alpha)\alpha] = 0 \tag{3}$$

where U_r is the velocity field for the compression interface and α is the volume fraction, which is defined as:

$$\begin{cases} \alpha = 0 & \text{air} \\ \alpha = 1 & \text{water} \\ 0 < \alpha < 1 & \text{free surface} \end{cases} \quad （4）$$

The finite volume method with unstructured grid is used to transform the equations from the physical space into the computational space. The solution of the governing equations is achieved by using the pressure implicit with splitting of operator (PISO) algorithm[7].

The dynamic overset grid is the key point for direct simulation of the complex motions with a hierarchy of bodies. Generally, an overset grid comprises two or more blocks of overlapping structured or unstructured grids, and the overset grids can move independently without constraints. In the dynamic overset computation process, the grids in the computational domain are first classified into types according to their locations, such as fringe cells, hole cells and donor cells etc. After digging holes, the grid in the non-computational domain will be excluded from computation. The overlapping area can transfer the flow field information by establishing interpolation relation.

The solver naoe-FOAM-SJTU used in this paper is based on the open source CFD software OpenFOAM platform as well as overset grid technology and multistage object motion solving module. When the flow field is soluted, the Suggar++[8] program is used to calculate the domain connectivity information (DCI) between the overset grids.

Geometry and simulation design

The KVLCC2 ship model with a single propeller is used for the numerical calculations since the rudder force during the stopping manoeuver is negligible, and the main geometric characteristics are listed in table 1.

Table 1: Main parameters of the ship model

	Full scale	Model scale
Length of waterline L/m	320.00	2.909
Width of waterline B/m	58.00	0.527
Draft d/m	20.80	0.189
Propeller diameter D/m	9.86	0.080
Propeller pitch ratio P/D	0.721	0.721

The computational domain is divided into three parts: one for the background grid, one for the grid around the ship hull and one for the grid around propeller. The unstructured grids are generated by snappyHexMesh with the background grid generated by blockMesh. The overset grid arrangement and the local mesh distribution is shown in figure.1.
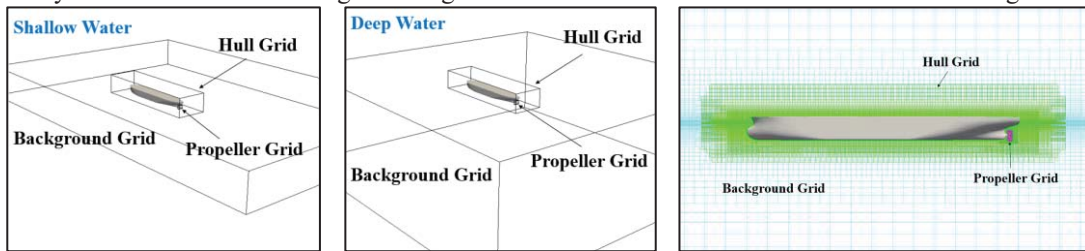

Figure 1 The overset grid arrangement and the local grid distribution

Test conditions

The simulation conditions are following the setup of experiments[9-10] performed at National Maritime Research Institute (NMRI). The simulation starts from the steady state of self-propulsion, with the speed of 0.4905 m/s in the case of model scale. Then the propeller is controlled to a reverse speed of -10.36r/s to carry on the stopping maneuver.

Numerical results and analysis

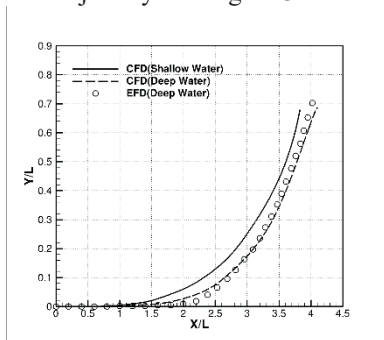Figure 2 shows the trajectory and Figure 3 shows the speed during the simulation time.

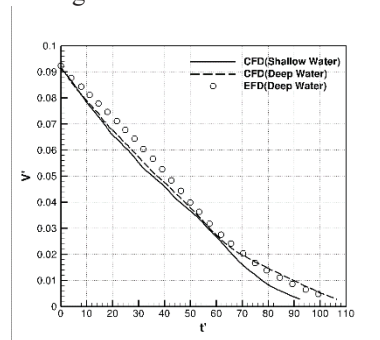**Figure 2 The ship trajectory**   **Figure 3 The ship speed**

Here the dimensionless length, velocity and time are used, which is defined as: $t' = t/\sqrt{L/g}$, $V' = V/\sqrt{gL}$, where L is the length of the ship and g is the acceleration of gravity.

The figure shows that the vertical distance and the horizontal distance of ship in deep water agree well with the experimental data. The vertical distance is 0.75% more than the experimental data, which is tend to be safe. While the horizontal distance is 4.29% smaller than the experimental data, which should be paid more attention in practical application. Meanwhile, the stopping time also agrees well with the experimental data. Therefore, the numerical calculation method used in this paper can accurately forecast the parameters of stopping maneuver.

The ship in shallow water has a shorter vertical distance and a shorter stopping time in comparison with those in deep water, while the horizontal distance is almost the same.

Figure 4 shows the total longitudinal force that act on the ship. And the total longitudinal force is decomposed to the hull resistance and the propeller force, as shown in Figure 5 and Figure 6 respectively.
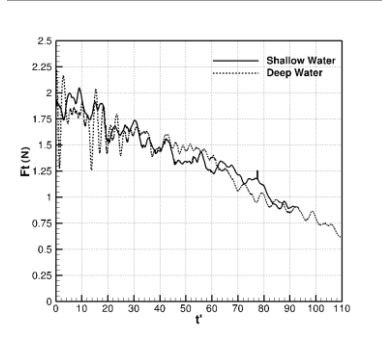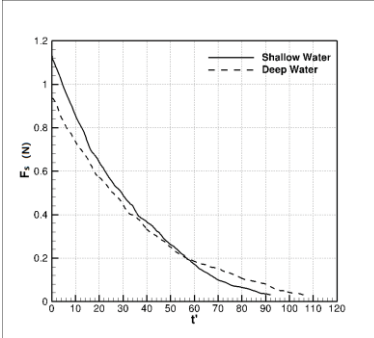

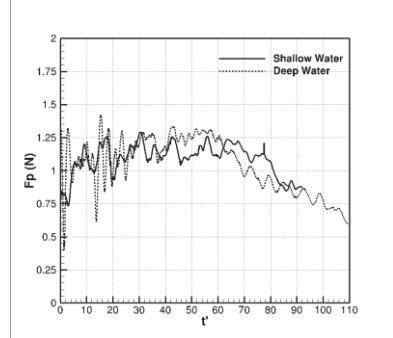**Figure 4 The total longitudinal force** **Figure 5 The hull resistance** **Figure 6 The propeller force**

Due to the continuous rotation of the propeller, the longitudinal force curve is fluctuating. It can be seen from the figure that the total longitudinal force gradually decreases as the ship speed decreases in accordance with the anticipation.

Figure 5 indicates that hull resistance Fs decreases when the speed decreases. When the speed is higher, the resistance of the hull in shallow water is greater than that in the deep water. From Figure 6, we can see that the propeller forces in different water depth are close to each other.

Figure 7 shows the pressure distribution on the side and the bottom of the ship. While figure 8 shows the distribution of flow velocity around the ship.
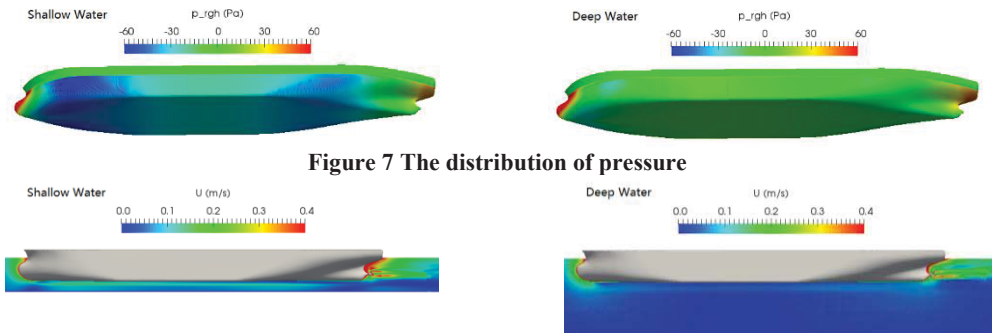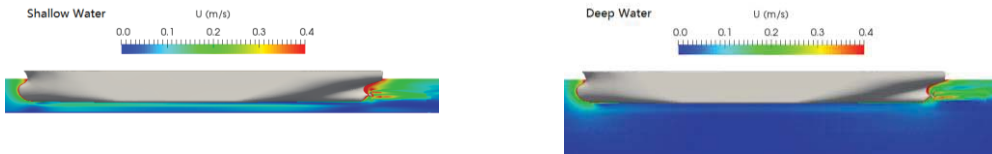

Figure 7 The distribution of pressure

Figure 8 The distribution of flow velocity

The figures indicate that when the ship is sailing in shallow water, the pressure on its side and bottom is smaller than that in deep water. Worse more, the pressure reduce will lead to the sinking of the ship, which increases the area of wetted surface, further increasing the friction resistance. Because the depth of freedom of the hull is fixed in this work, the shallow water effects is not so serious compared with the actual situation.

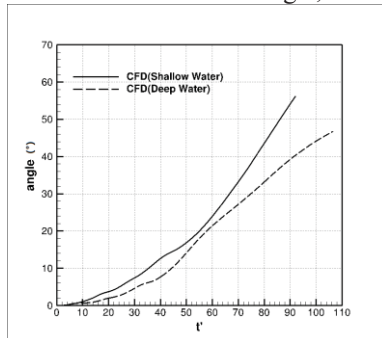Figure 9 shows the time travel of bow angle, while Figure 10 shows the turning moment.

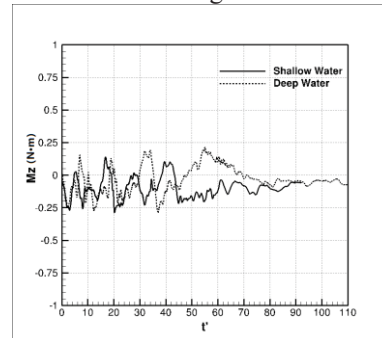**Figure 9 The bow angle** **Figure 10 The turning moment**

Figure 9 shows that the yaw angle in shallow water is larger through the whole process. When the ship is completely stopped, the deflection angle is 56.2 degrees. While the ship in deep water ends with the 46.3 degrees deflection angle. In shallow water, the ship model reaches a greater deflection angle with less time.

From Figure 10, it is found that the value of moment fluctuates greatly because of the dynamic working state of the propeller. The average value of moment after the propeller began to reverse in shallow water is 0.121 N·m, when it was 0.068 N·M in deep water. With the same reverse speed of propeller, the turning moment in shallow water is slightly larger, leading to greater yaw motion.

Figure 11 and Figure 12 show the distribution of pressure on the stern and velocity on horizontal section around the propeller both in shallow and deep water when the ship speed decreased to 50% initial value.
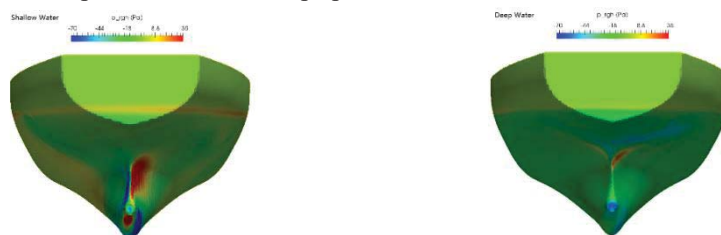

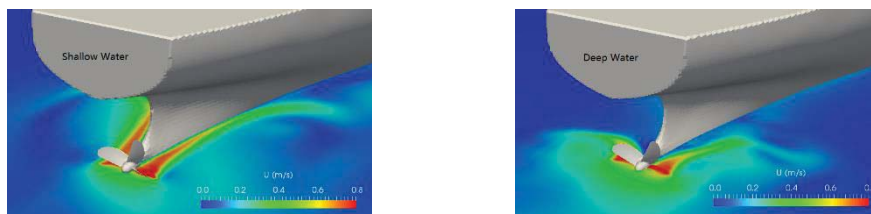**Figure 11 The distribution of pressure**

Figure 12 The distribution of flow velocity

It can be seen from Figure 11 that a high pressure area presents on the right aft of the ship because of the reversing propeller. The pressure pushes the ship tail to the left, which makes the ship turn right. In shallow water, the high pressure is more prominent, thus increasing the turning moment.

Figure 12 shows how reversing propeller works during the stopping maneuver. The water is propelled to the front, and the reaction force help the ship to decelerate. In shallow water, more liquid is propelled forward because the space below is restricted. More water pushes the hull, leading to larger lateral force and turning moment.

Although the effect of shallow water can provide some benefit to stopping maneuver as reducing the longitudinal distance, it is still very limiting. In addition, more attention is supposed to be paid to the increases of horizontal distance and yaw angle.

Acknowledgements

References

[1] CHISLETT M S, SMITT L W. A brief description of the hya large amplitude pmm system[J]. ARCHIVE Journal of Mechanical Engineering Science 1959-1982 (vols 1-23), 1972, 14(7):80-84.

[2] SAKAMOTO N, CARRICA P M, STERN F. URANS simulations of static and dynamic maneuvering for surface combatant: Part 2. Analysis and validation for local flow characteristics[J]. Journal of Marine Science and Technology, 2012, 17(4): 446-468.

[3] CARRICA P M, STERN F. DES simulations of KVLCC1 in turn and zigzag maneuvers with moving propeller and rudder[C]. Proceedings of the SIMMAN 2008 Workshop on Verification and Validation of Ship Manoeuvering Simulation Methods. Lyngby, Denmark, 2008.

[4] SHEN Z R, WAN D C. Manual of CFD solver for ship and ocean engineering flows: naoe-FOAM-SJTU. Technical Report for Solver Manual, Shanghai Jiao Tong University, 2014.

[5] WANG J H, WAN D C. Investigations of Self-Propulsion in Waves of FullyAppended ONR Tumblehome Model[J]. Applied Mathematics and Mechanics, 2016, 27(12):619-623.

[6] RUSCHE H. Computational Fluid Dynamics of Dispersed Two-Phase Flows at High Phase Fractions[D]. Imperial College London (University of London), 2003.

[7] CAO H, WAN D C. Benchmark computations of wave run-up on single cylinder and four cylinders by naoe-FOAM-SJTU solver[J]. Applied Ocean Research, 2017, 65: 327-337.

[8] NOACK R W, BOGER D A, KUNZ R F, CARRICA P M. Suggar++: An improved general overset grid assembly capability[C], Proceedings of the 47th AIAA Aerospace Science and Exhibit, San Antonio TX, 2009, 22-25.

[9] TSUKADA Y, UENO M, TANIZAWA K. Development of an Auxiliary Thruster for Free-running Model Ship Tests[J]. Journal of the Society of Naval Architects of Japan, 2014, 20:59-67.

[10] UENO M, SUZUKI R, TSUKADA Y. Estimation of stopping ability of full-scale ship using free-running model[J]. Ocean Engineering, 2017, 130:260-273.